Bonn zoological Bulletin 72 (2): 223–233
2023 · Schmied H. et al.
https://doi.org/10.20363/BZB-2023.72.2.223

ISSN 2190–7307
http://www.zoologicalbulletin.de

Research article
urn:lsid:zoobank.org:pub:B1045D56-14E5-48BD-B8CE-81C6AD15D215

Functional morphology of water holding by feathers of sandgrouse (Aves: Pteroclidae): first evidence for directed hydroscopic motion in animals

Heiko Schmied [1,*], David Klocke [2] & Alexander Rüttgers [3]

[1] *Institute of Crop Science and Resource Conservation, Agroecology and Organic Farming Group, University Bonn, Auf dem Hügel 6, D-53121 Bonn, Germany*
[2] *Institute of Zoology, University of Bonn, Poppelsdorfer Schloss, Meckenheimer Allee 169, D-53115 Bonn, Germany*
[3] *Institute for Software Technology, High-Performance Computing Department, German Aerospace Center (DLR)*

* *Corresponding author: Email: schmied@uni-bonn.de*

[1] urn:lsid:zoobank.org:author:23854168-99EA-4DE5-A56A-CAF810D3C26B
[2] urn:lsid:zoobank.org:author:CF4F1E74-7E31-45A4-A6A4-C461136A03DB
[3] urn:lsid:zoobank.org:author:F84A3DD1-A646-46F8-8A70-4E6A92E7590D

Abstract. The water transport of sandgrouse (Pteroclidae) presents one of the most amazing behaviors in birds. The unique ability to absorb water by their abdominal feathers was disclaimed over decades but is described here for the first time. For a comprehensive picture of the morphological and physical parameters, we used different approaches in pterylography, functional morphology, biomechanics, new measurement techniques and calculations of wetting properties, absorption capacity tests and numerical simulations. We show that the ability of carrying large amounts of water is caused by different factors like: the distribution of feathers on the underside, a specialized feather margin, a well-directed hygroscopic alteration of the microstructure, which is the first discovered in the animal kingdom and a unique hydrophilicity of the feather material. Determination of absorption capacities of feathers in sandgrouse and non-sandgrouse species clearly shows the effects of the different adaptations in feather structure. Numerical simulations determine the adhesive force of the feather microstructure of sandgrouse and show that minimal changes of the structure lead to a complete loss of the specialized properties. From this we conclude that the microstructure of sandgrouse feathers has evolved to absorb the largest possible volume of water with as little material as possible. Our results show that the water transport in sandgrouse is based on the interaction of many highly derived characteristics.

Key words. Sandgrouse, *Pterocles*, biomechanics; contact angle; wettability; hygroscopic motion.

INTRODUCTION

Sandgrouse (Pteroclidae) mostly live in arid areas and feed nearly exclusively on dry seeds so in consequence they need to drink daily (MacLean 1983; de Juana 1997; Lloyd et al. 2000). Because sources of surface water are up to 80 kilometers away from the nesting sites (MacLean 1968), the young depend on their parents for drinking (de Juana 1997). Therefore, the males of all sandgrouse species, except of the Tibetan Sandgrouse (*Syrrhaptes tibetanus*), absorb water with their abdominal feathers (on average 25 ml for males, less for females; Cade & MacLean 1967) and fly to their young that drink out of the parents' plumage (Cade & MacLean 1967; MacLean 1983; de Juana 1997). This behavior was disowned as a myth by ornithologists over decades in the twentieth century until Cade & MacLean (1967) firstly documented this behavior in the wild. The so-called belly-soaking of the Charadriidae is similar to the water transport of sandgrouse. If temperatures are very high at their breeding sites, adult birds wet their belly feathers and then sit on the clutch or nestlings (MacLean 1975). The behavior was interpreted as cooling the eggs, the nestlings and/or the breeding adult bird (Maclean 1975, Seymour & Ackerman 1980, Amat & Masero 2007, 2009). Sporadically this behavior also occurs in other bird families, e.g., in the Sternidae (Grant 1981), Rhynchopidae (Strong & Miyako 2004), Recurvirostridae (Goutner 1984) and Hirundinidae (Jackson & Schardien 1981). Belly-soaking often only occurs during particularly hot periods (Begg & Maclean 1976). However, it has never been described that young birds ingested water. In addition, the feather structures of plover species do not show any characteristics that indicate specialization for water absorption (own data, unpublished). In sandgrouse the feather microstructure of specialized abdominal feathers changes by wetting. Rijke (1972) and Joubert & MacLean (1973) tried to explain this process by a molecular change of keratin but could not give a biomechanical explanation for the microstructural movement. Therefore, the explanation for the extraordinary wetting properties and the physical basis for the efficiency of water transport are still unknown.

Received: 26.05.2021
Accepted: 24.11.2023

Corresponding editor: T. Töpfer
Published: 28.11.2023

We used different kinds of morphological, physical and numerical approaches to explore the water transport of sandgrouse. The pterylography of sandgrouses and some species of pigeons (Columbidae), their close relatives, was studied to clarify whether the distribution and orientation of the feathers is already specialized in water transport, which was not considered by former studies. We investigated the feather morphology of nine sandgrouse and four none-sandgrouse species macro- and microscopically. This enabled us to compare variations in feather structure within the Pteroclidae (including *S. tibetanus*) and to demonstrate differences to closely related land birds (Pigeons, sister taxon of the Pteroclimesites [Sandgrouse & Mesites]; Sangster et al. 2022), unrelated land birds (Finches, Fringillidae) as well as bird taxa which always get in contact with water (Grebes, Podicepididae and Cormorants, Phalacrocoracidae). To describe the mechanism of water transport we examined the change in the internal structures of the feathers when they were wetted.

The internal composition of the barbules was investigated by semi-thin sections, freeze fractures and scanning electron microscope (SEM) to understand the microstructural movements. Furthermore, the biomechanical properties of different parts of the feather material were directly measured by atomic force microscopy under dry and wet conditions. The wetting properties of feathers were described by direct measurements of the material contact angle in sandgrouse and non-sandgrouse species. Calculations of the intrinsic contact angle were made (according to Cassie & Baxter 1944; Wenzel 1936) to explain the different wetting properties adapted to the birds' mode of life. We measured the different water absorption capacities of complete and experimentally modified sandgrouse feathers as well as feathers from non-sandgrouse species according to Thomas & Robin (1977). This enabled us to compare the morphology and wetting properties with water intake and to test the hypothesis that water absorption of sandgrouse feathers follows the Michaelis-Menten saturation curve. To understand the intensity of the adhesive forces inside the sandgrouse microstructure when wetted, we generated numerical simulations with an original and a varied morphology and observed their ability to retain water droplets against gravity. For terminology of feather microstructure we refer to Sick (1937) and Dove (1997).

MATERIALS AND METHODS

(a) Pterylography

Feathers were plucked on the ventral side of one dead specimens of Namaqua Sandgrouse (*Pterocles namaqua*), of several partial skins of Double-banded Sandgrouse (*P. bicinctus*) and of one Common Wood Pigeon (*Columba palumbus*) from the Zoological Collection of the Department Animal Ecology (University of Bonn). The number of breast and belly feathers and their orientation were recorded. Distributions of feather tracts (pterylae) were drawn.

(b) Feather morphology

Several breast feathers of males (in some species also of females) of nine sandgrouse species (*P. namaqua, P. bicinctus, P. burchelli, P. exustus, P. guttularis, P. orientalis, P. quadricinctus, P. lichtensteinii, Syrrhaptes tibetanus*) and other non-sandgrouse species [Common Wood Pigeon, Cormorant (*Phalacrocorax carbo*), Grosbeak (*Coccothraustes coccothraustes*), Little Grebe (*Tachybaptus ruficollis*)] were photographed (Nikon D40x) and examined regarding their microstructure by stereomicroscope (Zeiss Discovery V12 SteREO with AxioCam Icc 3).

Several breast feathers of *P. namaqua*, *P. bicinctus* as well as of Common Wood Pigeon, Cormorant, Grosbeak and Little Grebe were scanned using a scanning electron microscope (Hitachi S-2460N) at the Zoological Research Museum Alexander Koenig (Bonn). Measurements of the microstructures were made using ImageJ ver. 1.42.

Feather samples of *P. exustus, P. guttularis, P. orientalis, P. quadricinctus, P. lichtensteinii* originated from the Bavarian State Collection of Zoology (Munich); *P. burchelli, Syrrhaptes tibetanus* from the Zoological Research Museum Alexander Koenig (Bonn); *C. coccothraustes* from the Institute of Zoology (Bonn); *T. ruficollis* from the Dresden Zoo and *Phalacrocorax carbo* from the Department Animal Ecology (see above).

(c) Changes in feather configuration by wetting and structure of the barbules

Several breast feathers of *P. namaqua*, *P. bicinctus* and comparison species (see above) were submerged in distilled water and examined dry and wet by stereomicroscopy.

Semi-thin sections of sandgrouse barbules (*P. namaqua*, *P. bicinctus*) were made by microtome cuts (Microm HM 360) after embedding in synthetic resin (Epon® 812-Ersatzprodukt). The sections were stained with methylene blue azure or toluidine blue fuchsine and were examined for their internal structure under microscope (Zeiss Axioskop with AxioCam MRc).

For the freeze fracture process, wet breast feathers of *P. namaqua* were dipped into liquid nitrogen, crushed by a mortar and additionally well dried. Fractions at the basal part of the barbules were investigated by SEM (see above).

Serval ultrasonic cleaned *P. namaqua* feathers were embedded in synthetic resin (Epoxydharz L, R&G Faserverbundwerkstoffe GmbH) and cut by microtome (Reichert OmU3 with a diamond knife) at an angle of 90° to the longitudinal axis of the barbules. The cross-section

surfaces of barbules were scanned by an atomic force microscope (Dimension 3100, Digital Instruments) under dry and wet conditions at the Institute of Zoology (Bonn) according to Klocke & Schmitz (2012).

(d) Wetting properties

For the measurement of the material contact angle θ, 6–8mm long tips of untreated apical barbs of *P. bicinctus, Phalacrocorax carbo* and *C. coccothraustes* were used. Additional samples of *C. coccothraustes* were dipped in acetone for a minute. Measurements of θ were made by a tensiometer (DCAT 21, DataPhysics Instruments GmbH) at the Institute of Textile Technology and Process Engineering (Denkendorf). Statistical analyses were made with OpenOffice Calc ver. 3.3.

For the calculating of the intrinsic contact angle θ*, measurements of the feather vane microstructure of *P. bicinctus, Phalacrocorax carbo*, *C. coccothraustes,* Bullfinch (*Pyrrhula pyrrhula*), Common Swift *(Apus apus)*, Cockatiel (*Nymphicus hollandicus*) were made by stereo microscope (see above) and ImageJ ver. 1.42. For measuring lengths on microstructure [2r = diameter of barbs; 2d = distance between barbs, according to Rijke (1970); h = height of barbs (only in *P. bicinctus*)] see Fig. 1B. The formula established by Rijke (1970) [(r+d)/r] for the estimation of structural wetting properties of bird feathers was calculated for every taxon based on average measurements of several feathers per species. Surface roughness (r` = proportion of real surface in contrast to geometrical projected surface) was calculated for *P. bicinctus* (without barbules) based on the specified measuring distances (see above). Calculations for the actual contact angle on feathers with heterogeneous wetting (Fig. 1A; *Phalacrocorax carbo*, *C. coccothraustes*, *Pyrrhula pyrrhula*, *Apus apus*, *Nymphicus hollandicus*) were made by the formulas (*a–c*) of Cassie & Baxter (1944):

$$a)\ \cos\theta^* = f_s \cos\theta - f_a$$
$$b)\ f_s = ((\pi r/(r+d))\,(1-\theta^*/180°)$$
$$c)\ f_a = 1-r \sin\theta\,/(r+d)$$

Calculations of θ* for feathers with homogeneous wetting (Fig. 1B; *P. bicinctus*) were made by the formula (*c*) of Wenzel (1936):

$$c)\ \cos\theta^* = r' \cos\theta$$

Feather samples of *Pyrrhula pyrrhula*, *Apus apus* and *Nymphicus hollandicus* originated from the Institute of Zoology (Bonn).

(e) Water absorption capacity

Breast feathers of *P. namaqua* (natural), *P. namaqua* (with the feather margin removed), *P. bicinctus*, Common Chaffinch (*Fringilla coelebs*), Domestic Canary (*Serinus serinus* forma *domestica*), House Sparrow

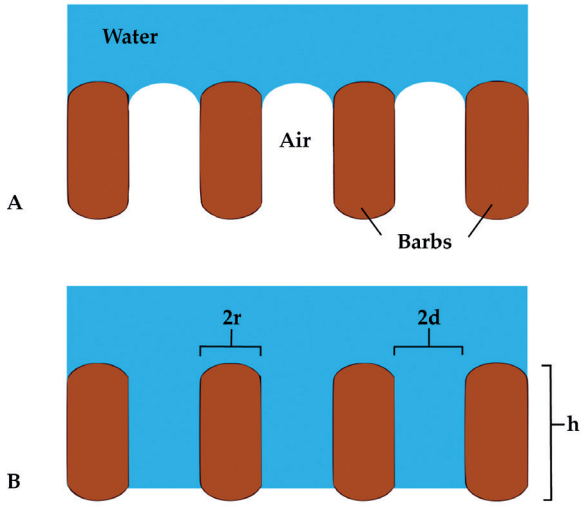

Fig. 1. Schematic cross section of wetted feather barbs (without barbules) with different wetting properties. **A**. Heterogeneous wetting with air pillows between the barbs (according to Cassie & Baxter 1944). **B**. Homogeneous wetting (according to Wenzel 1936). Measurements of microstructures (2r, 2d, h) are indicated.

(*Passer domesticus*), Yellowhammer (*Emberiza citrinella*), *Pyrrhula pyrrhula*, *C. coccothraustes*, Great Spotted Woodpecker (*Dendrocopos major*) and *Nymphicus hollandicus* were used for the determination of absorption capacity over time (15 s, 30 s, 60 s, 120 s and 240 s in distilled water) according to Thomas & Robin (1977). In contrast to Thomas & Robin (1977) the feathers were replaced on the water surface with the ventral side to get a more uniform wetting because of different curvature of the feathers. For weighing a micro scale (KERN AEJ 220-4M) was used. Statistical analyses were made by OpenOffice Calc ver. 3.3.

Feather samples of *Fringilla coelebs*, *Serinus serinus* forma *domestica, Passer domesticus* and *Dendrocopus major* originated from the Institute of Zoology (Bonn). Samples of *Emberiza citrinella* originated from the Department Animal Ecology (Bonn).

(f) Numerical simulation

For modelling the adhesive forces in the sandgrouse's breast feathers, we built a computer model of the microstructure geometry (barbs and barbules in wet orientation, Fig. 2A–C) on the basis of the morphological description (see below). Then a falling water drop (volume: 0.034 mm^3; initial velocity of fall: 0.5 m/s; note that this initial velocity is below the terminal velocity of a water droplet with the same volume) was inserted for a three-dimensional flow simulation (Fig. 2E). Furthermore a modified geometry with 30% less barbules was created and tested in the same way (Fig. 2D). For performing the simulation, we used the two-phase flow solver NaSt3DGPF (Croce et al. 2010). For the discretisation of the Navier-Stokes equations, NaSt3DGPF employs a high-order

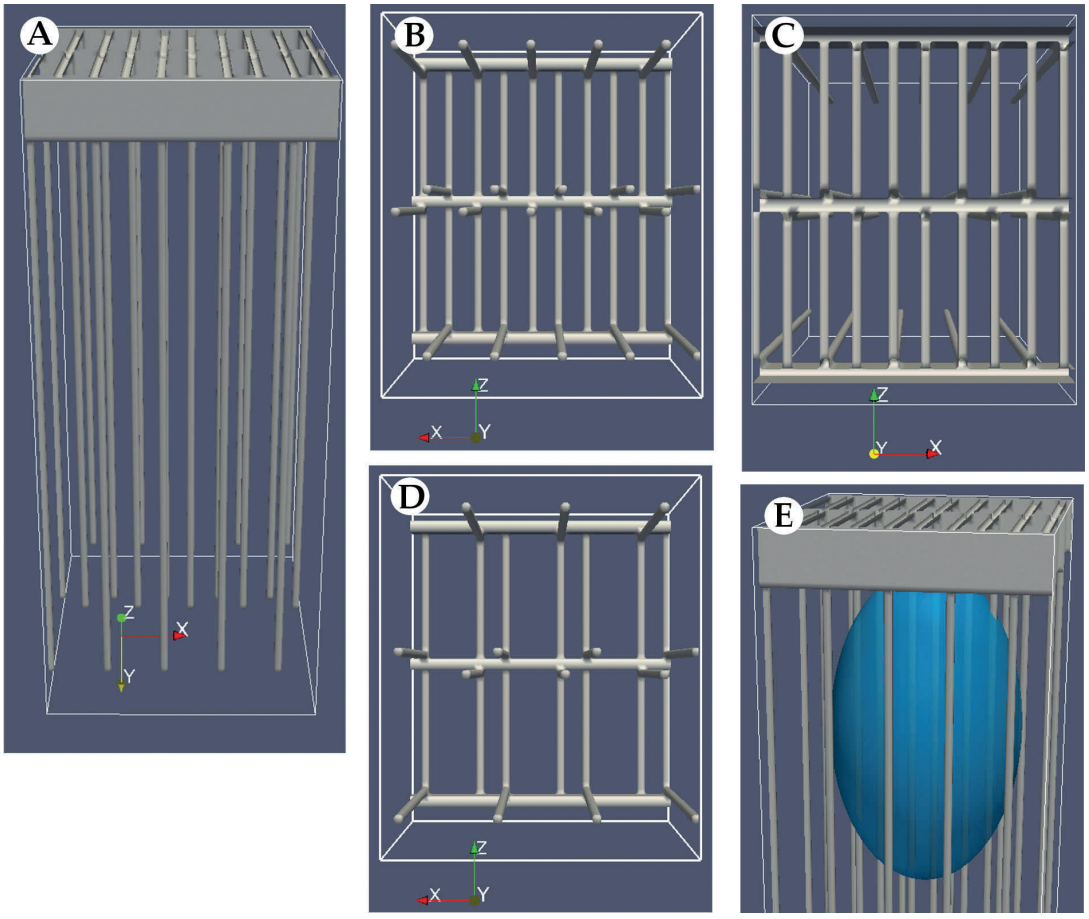

Fig. 2. Simulation space (0.5 × 1.2 × 0.6 mm) with inserted geometries. **A–C**. Sandgrouse microstructure geometry. **A**. Lateral view. **B**. Ventral view. **C**. Dorsal view. **D**. Ventral view on the varied geometry contains 30% less barbules. **E**. Initial conditions of the three-dimensional flow simulation with inserted water droplet inside the sandgrouse's microstructure geometry (lateral field of view).

finite difference method on a staggered grid in space and a third-order Runge-Kutta method in time. The two fluid phases are distinguished with the levelset technique and surface tension is modeled with the Continuum Surface Force (CSF) method. The flow solver is parallelized with MPI and with Nvidia's CUDA architecture to reduce computing time. The visualization was performed by ParaView ver. 3.1.4. We analyzed qualitative data such of droplet's barycenter position, its initial velocity and gave a measurement for the droplets' deformation in the two specified geometries over time.

RESULTS

(a) Pterylography

The pterylography of *P. namaqua* and *P. bicinctus* differs from that of *Columba palumbus* in the distribution and in the form of feather tracts (Fig. 3A–B). On the ventral side, about 1100 feathers were counted in sandgrouse (16 cm head-torso length) and about 830 in *C. palumbus* (22.8cm head-torso length). About 380 of the sandgrouse's feathers exhibit specialized characteristis for water transport. They are localized around the featherless area in the middle of the breast and belly (Fig. 3A). Specialized feathers of sandgrouse are oriented in clearly demarcated rows towards the featherless region whereas pigeon feathers are relatively evenly distributed and usually oriented caudally.

(b) Feather morphology

The breast feathers of sandgrouse (e.g., *P. namaqua*; Fig. 3C–D) differed from other body feathers by an elongated shape and by a distinct outer rim (unconnected distal ends of the barbs). In *S. tibetanus* (Fig. 3E) the breast feathers exhibit a reduced pennaceous vane and a large indistinct outer rim. Back feathers from *P. namaqua* (Fig. 3F) and other sandgrouse-species show a broad uniform vane and plumulaceous basis. Breast feathers of non-sandgrouse species show a large range of different morphologies (Fig. 4). Feathers of *C. palumbus* exhibit a large plumulaceous part and a relatively small pennaceous vane whereby in many cases the pennaceous region is completely lost. In *C. coccothraustes* feathers a large

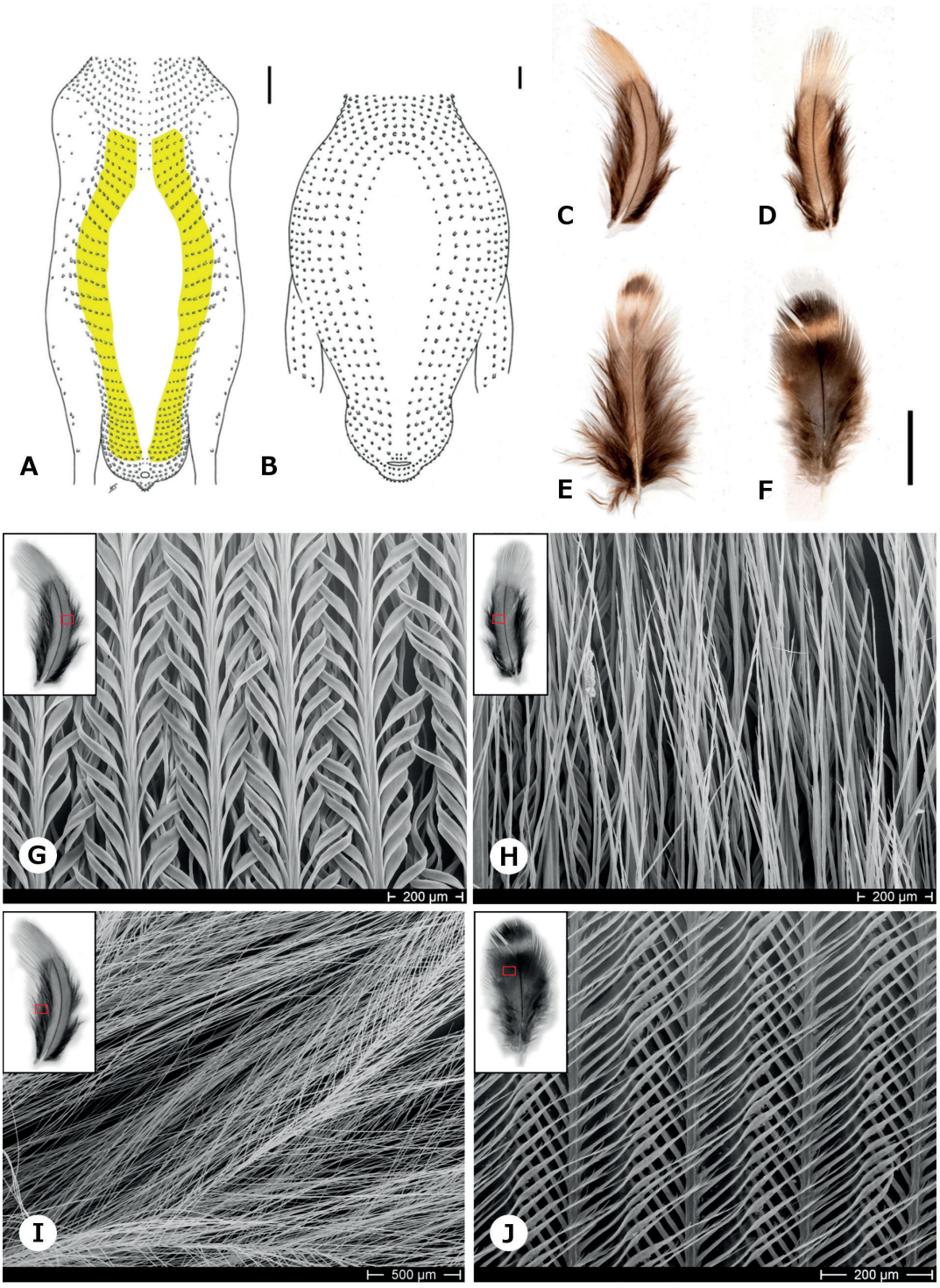

Fig. 3. A. Schematic pterylography of the breast and belly region of *P. namaqua* by means of follicle distributions. **B**. Schematic pterylography of the breast and belly region of *C. palumbus* by means of follicle distributions. **A–B**. Regions with follicles of specialized feathers for water transport are marked in yellow. **C–F**. Different body feathers of sandgrouse. **C**. Elongated breast feather of *P. namaqua*, dorsal view, with distinct outer rim. **D**. Elongated breast feather of *P. namaqua*, ventral view, with distinct outer rim. **E**. Dorsal view on breast feather of *S. tibetanus* with reduced pennaceous vane and indistinct outer rim. **F**. Back feather of *P. namaqua* with a uniform pennaceous vane and plumulaceous basis. **G–J**. SEM pictures of *P. namaqua* feather microstructure. **G**. Breast feather vane, dorsal view. **H**. Breast feather vane, ventral view. **I**. Loose barbs and elongated barbules of the outer rim of a breast feather, dorsal view. **J**. Microstructure of barbs and barbules (with and without barbicels) of a back feather vane, dorsal side. Scale bars: A–F = 1cm.

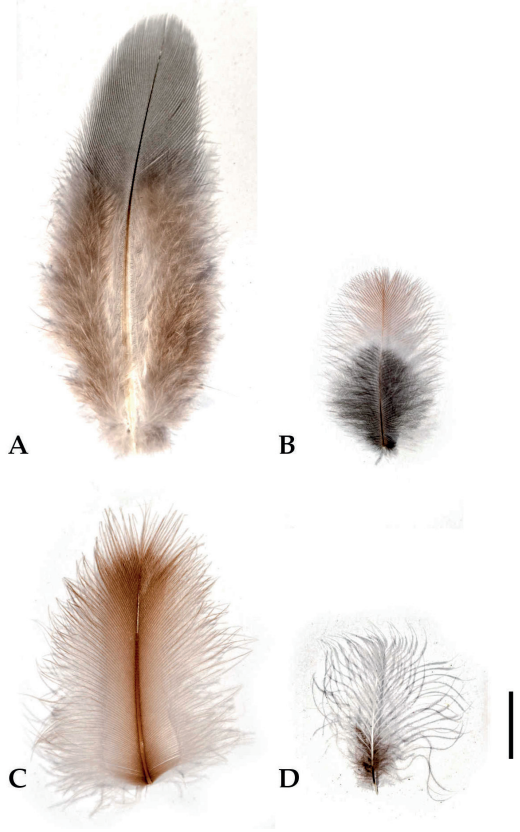

Fig. 4. Breast feathers in dorsal view. **A**. *C. palumbus*. **B**. *C. coccothraustes*. **C**. *P. carbo*. **D**. *T. ruficollis*. Scale bar = 1 cm.

plumulaceous part is present, too. *P. carbo* breast feathers show a continuous slender pennaceous vane with a broad outer rim. The feathers of *T. ruficollis* are very loose and show no connected vane.

The microstructure of the pennaceous region of the breast feathers of male sandgrouse (as well as in the few examined females) differs from that of other birds. The inner part of the vane is built by homogenous barbules which are intertwined by a twisted basis (Fig. 3G). The number of whorls differs by species and range in males on average from one (*S. tibetanus*), two (*P. quadricinctus*, *P. lichtensteinii*, *P. bicinctus*), three (*P. burchelli*, *P. exustus*, *P. guttularis*, *P. namaqua*) up to five (*P. orientalis*). The barbules are elongated (1mm in length), exhibit no barbicels and protrude from the ventral side of the feather vane (Fig. 3H) at an angle of 20°. In contrast, the outer rim consists of loose barb ends with elongated and completely straight barbules (Fig. 3I). The microstructure of the sandgrouse's back feathers exhibit barbules with and without barbicels which are interlocked (Fig. 3J) and resembles the normal structure of a pennaceous feather vane like breast feathers from *C. palumbus* or *C. coccothraustes*. *P. carbo* show a very fine-mesh inner vane of the same composition and a distinct outer rim with loose barbs and barbules. *T. ruficollis* exhibits uniform barbules without barbicels and a simple twisted basis which are not interlocked into each other. Feather microstructures of comparison species are shown in Fig. 5.

(c) Changes in feather configuration by wetting and structure of the barbules

The wetting changed the configuration of the morphology of the sandgrouse feathers in all species. The outer rim of the vane turned down to the ventral side of the feather (Fig. 6A) and formed a tube around the absorbed water. Only in *S. tibetanus* this mechanism was incomplete because of the broad and indistinct outer rim. The whorls at the basis of the barbules (Fig. 6B) unrolled by the contact with water (Fig. 6C) and changed the angle of the barbules to the feather vane on the ventral side from ca. 20° to ca. 90°. Both morphological changes from dry (Fig. 6D) to wet conditions (Fig. 6E) built a 3D-net of filamentous structures for storage of a large volume of water inside the feather structure. Both changes were completely reversible by drying. In *C. palumbus*, *C. coccothraustes* and *P. carbo* no morphological changes were observed in the feather structure by wetting. Barbules of *T. ruficollis* also unrolled their mono-twisted basis by contact with water but hardly changed their angle in relation to the feather vane.

The structure of the barbules (Fig. 6F) varied along their length. The medial and apical parts (Fig. 6G) showed a circular cross section with an outer layer and partly dark core coloration. The basal part of the barbules exhibited a crescent-shaped cross section (Fig. 6H) with an outer layer and two distinct inner layers with different structures. The keratin fibers of the layer of the concave side run in an angle of 90° to the fibers in the layer of the convex side. In SEM-pictures of freeze fractures from the basal part of barbules (Fig. 6I) an outer layer is not visible. The surface of the concave side of the basal part of the barbules has a fine dashed structure (Fig. 6I) in contrast to an amorphous shaped surface on that of the convex side (not shown).

Atomic force microscopic scans of cross sections from the basal part of the barbules (Fig. 6J) show two distinct layers, one at the convex side and another at the concave side. The two layers differ in their surface structure. In dry condition, the surface of both layers shows only minor differences in height of about 100nm (Fig. 6K–L). In wet condition the surface of the convex side raises up to ca. 500nm above the surface of the concave side (Fig. 6M–N).

(d) Wetting properties

The average material contact angle θ of breast feathers of *P. bicinctus* is 83.6° (n=13), of *P. carbo* 92.8° (n=14) and of untreated *C. coccothraustes* 96.5° (n=14). *C. coccothraustes* feathers which were dipped in acetone show a material contact angle of 94.5° (n=17) (Fig. 7A). Except for the hydrophilic sandgrouse feathers (θ = below

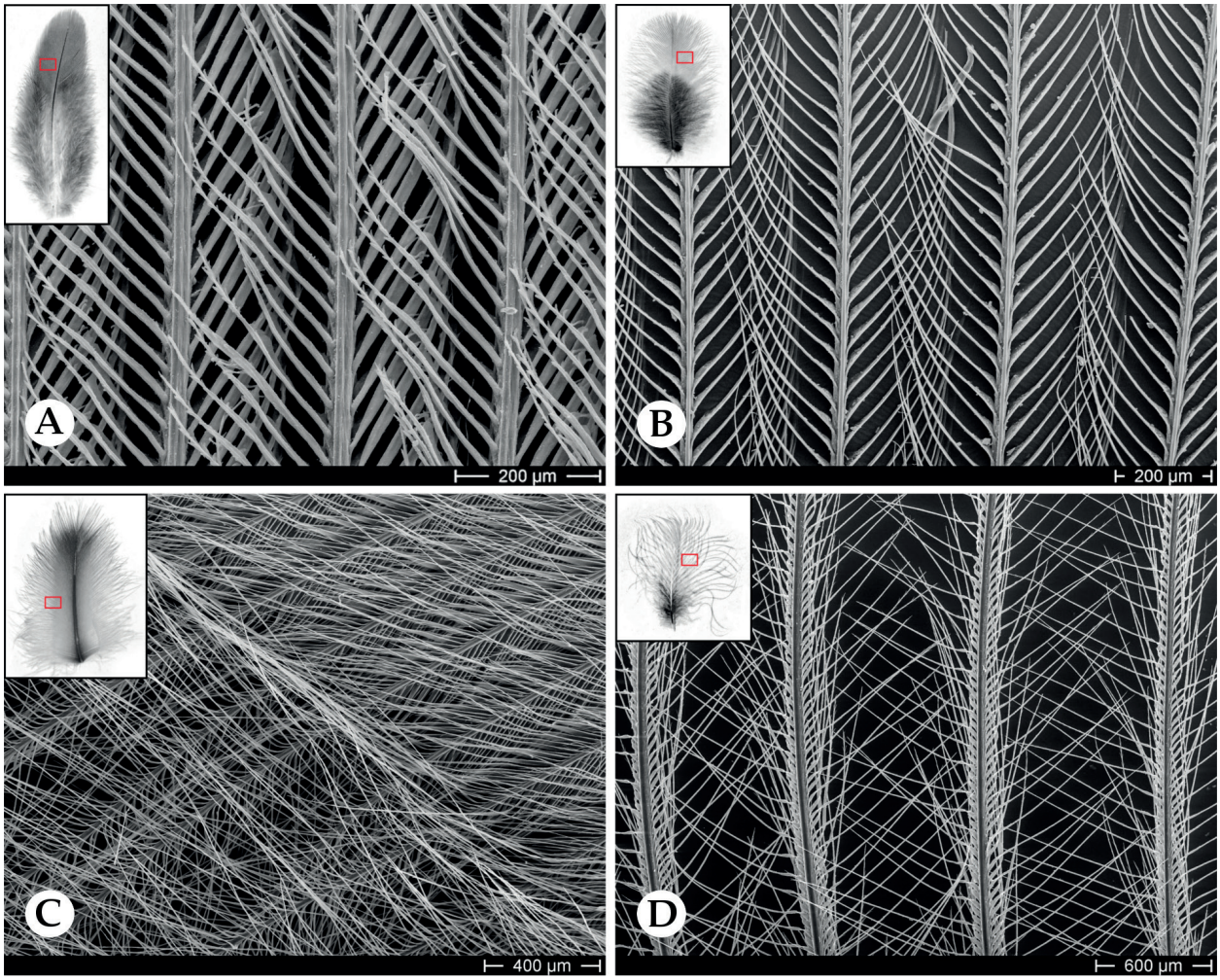

Fig. 5. Breast feather microstructure (barbs and barbules) in dorsal view. **A**. *C. palumbus*. **B**. *C. coccothraustes*. **C**. *P. carbo*. **D**. *T. ruficollis*.

90°), all material contact angles were hydrophobic (θ = over 90°). The contact angle of the sandgrouse differs significantly (two-tailed t-test, $p < 0.05$) from those of *P. carbo* and both *C. coccothraustes* samples.

Structural parameters and calculated (r+d)/r values of sandgrouse and non-sandgrouse species are listed in Table 1. The surface roughness r` of *P. bicinctus* breast feathers is 1.83 (706.650 µm² = real surface; 385.650 µm² = geometrical projected surface). Calculations based on the material contact angle θ and on the structural parameters resulted in the intrinsic contact angle θ* for all species (Table 2). Except for the hydrophilic sandgrouse feathers

Table 1. Structural parameters (n = 15) of breast feather microstructure parameters according to Rijke (1970).

species	2r (in µm)	2d (in µm)	(r+d)/r	h
P. carbo (inner vane)	37.4	238.1	7.4	
P. carbo (outer rim)	33.1	352.3	11.7	
C. coccothraustes	24.9	257	11.3	
P. pyrrhula	21.4	240.8	12.2	
N. hollandicus	23.3	231.8	11	
A. apus	19.1	227.3	12.9	
P. bicinctus	17.1 (n = 8)	240 (n = 10)	15	107 µm (n = 13)

Table 2. Material θ and intrinsic contact angle θ* plus wetting properties of breast feathers according to calculations after Cassie & Baxter (1944) and Wenzel (1936).

species	material contact angle θ	intrinsic contact angle θ*	wetting properties
calculations according to Cassie & Baxter (1944)			
P. carbo (inner vane)	92.8°	151°	hydrophobic
P. carbo (outer rim)	92.8°	150.6°	hydrophobic
C. coccothraustes (natural)	96.5°	157.9°	hydrophobic
C. coccothraustes (aceton)	94.5°	157.3°	hydrophobic
calculations according to Wenzel (1936)			
P. bicinctus	83.6°	78.2°	hydrophilic

(θ* = below 90°), all intrinsic contact angles were hydrophobic (θ* = over 90°).

(e) Water absorption capacity

Sandgrouse feathers (*P. namaqua*, *P. bicinctus*) show their maximum water absorption capacity after 15 s. In contrast to the entire feathers, the water absorption of the *P. namaqua* feathers without an outer rim is reduced by about 30%. Feathers from non-sandgrouse species exhibit a low and linear increase of water intake (Fig. 7B).

(f) Numerical simulation

In the simulations, the falling water droplet decelerated differently depending on geometry (Fig. 7C–D). In the sandgrouse geometry, the droplet's fall ended after about 1.1 ms. The droplet then deformed, due to surface tension, into a spherical shape in an upward direction. The droplet in the varied geometry was falling for the full simulated time of 1.8ms. The water droplet in the sandgrouse geometry lost 0.2 mm in height until the sinking process was stopped.

DISCUSSION

It took a long time to clearly demonstrate water transport in sandgrouse for the first time and the underlying functional morphology also remained obscure for long. The latter could now be explained using new investigation methods, in particular the atomic force microscope. However, only different methodological approaches together will provide a complete picture of the water intake of sandgrouse.

Our results showed that besides the feather structure the **pterylography** of the breast and belly may also have an influence on the total water holding capacity. In contrast to closely related pigeons, sandgrouse showed a higher number of feathers within the breast and belly parts which overlapped more and orientated towards the featherless region in the middle of the abdominal side to form a maximum volume of feathers in this body region. Nitzsch (1840) investigated the pterylography of sandgrouses and pigeons but found no relevant differences except for the parallel form of the ventral feather tracts in sandgrouse which we also found.

Former investigations illustrated the **specialized feather structure** (Cade & MacLean 1967, Joubert & MacLean 1973) but did not mention the outer rim and its function in the feathers nor could they explain the movement of the barbules. In this work we were able to confirm that the outer rim plays an important role in the water holding capacity and that the movement of the microstructure is based on a hydroscopic motion due to a different swelling of two inner keratin layers. Joubert & MacLean (1973) also supposed that water enters the keratin structure and changes the structural formation, but they could not explain the biomechanical process. Our result is the first evidence of a directed hydroscopic motion for animals which is already well known for plants. In plants, the swelling and de-swelling of dead cells creates a repeatable movement that usually serves to spread spores, pollen or seeds. Two differently arranged cell layers of a tissue, each with a given direction of expansion (swelling anisotropy), cause a curvature or torsion of the overall structure. Interestingly, the thread-like partial fruits of the heron's bill (*Erodium* sp.) are very similar to the specialized barbules of sandgrouse in that they also have a basal spiralization, which unrolls completely when wetted (Sitte et al. 1998).

The material **contact angle** is normally measured by an optical goniometer (Barthlott & Neinhuis 1997) but this is only possible on plane surfaces (Marmur 2006). For measuring the material contact angle of feathers a tensiometer was used for the first time which is an established method in textile research (Hofmann 2002). By using this technique, we could confirm that sandgrouse exhibit hydrophilic feathers in contrast to other birds (including the cormorant). The feather structure indicates

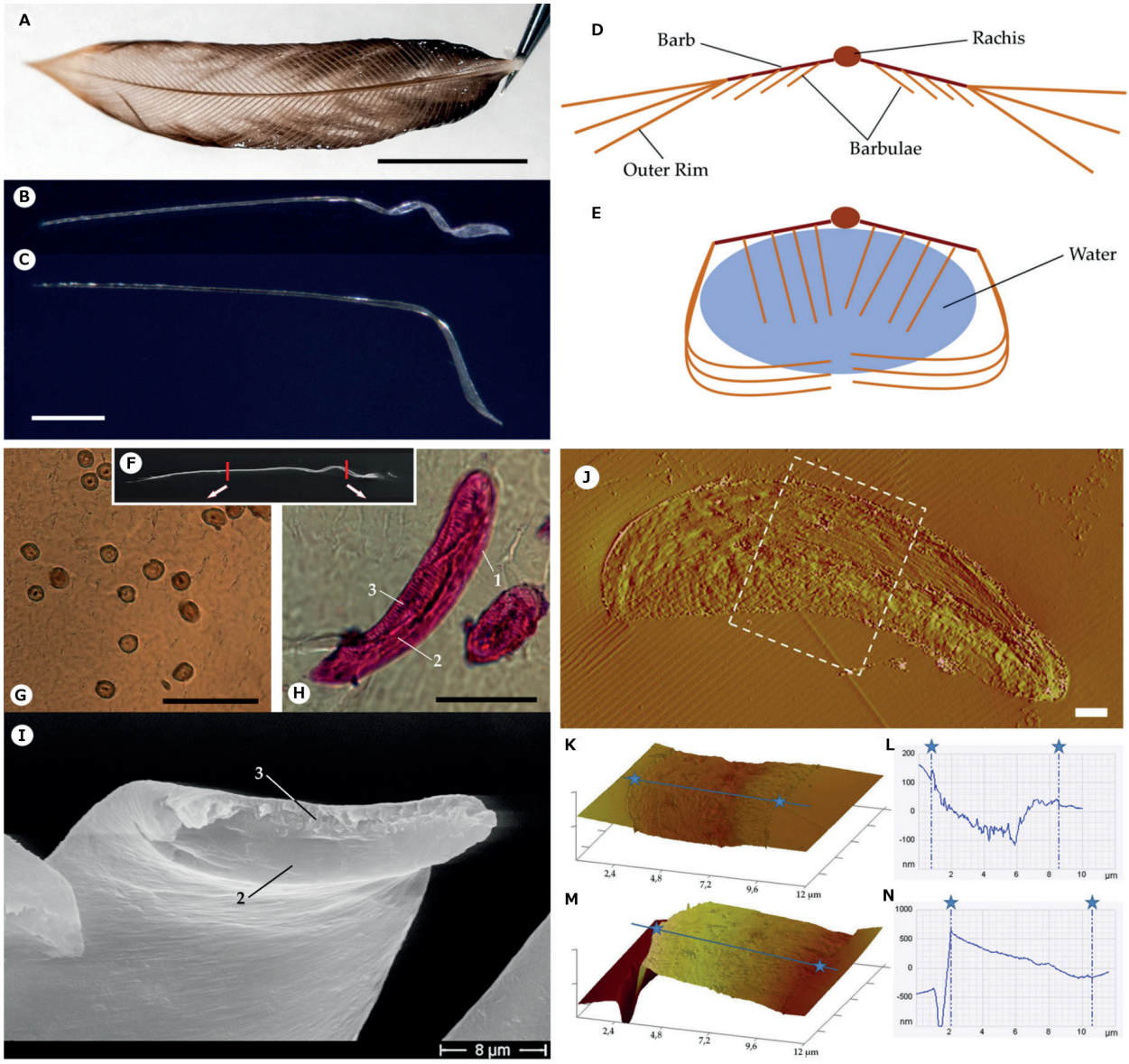

Fig. 6. A–E. Morphological changes in sandgrouse breast feathers. **A**. Outer rim of the vane turned down on the ventral side of the feather by wetting. **B**. Twisted basis of isolated barbule in dry conditions. **C**. Twisted basis of isolated barbule unrolled by contact with water. **D**. Idealized scheme of a feather in dry conditions. **E**. Idealized scheme of a feather in wet conditions. **F–I**. Internal composition of the barbules. **F**. Complete barbule with markings (red lines) of the cross section positions without scale. **G**. Light microscopic cross sections of the apical part of several barbules with distinct outer layers and partly dark core colorations (*P. namaqua*). **H**. Crescent-shaped cross section of the basal part of barbule with an outer layer (1) and two distinct inner layers (2 = concave side; 3 = convex side) with different fiber directions (*P. bicinctus*). **I**. SEM-picture of a freeze fracture of the basal part of the barbule without a visible outer layer and different surface structures of the breaking edges of the two inner layers. **J–N**. Atomic force microscope scans of the cross section of the basal part of a barbule (*P. namaqua*). **J**. Two-dimensional view on the surface structure in dry conditions with two distinct layers visible. White dashed square marks the area examined in K–N. **K**. Three-dimensional field of view of both layers when dry (three-dimensional view of the dashed field in J), with a corresponding height profile in L. **M**. Three-dimensional field of view of both layers when wet with a corresponding height profile in N. Line between the blue stars in K and M represents the respective path (through both layers) for the elevation profile in L and N. Scale bars: A = 0.5 cm; B–C = 200 µm; F–G = 50 µm; H = 20 50 µm; J = 2 µm.

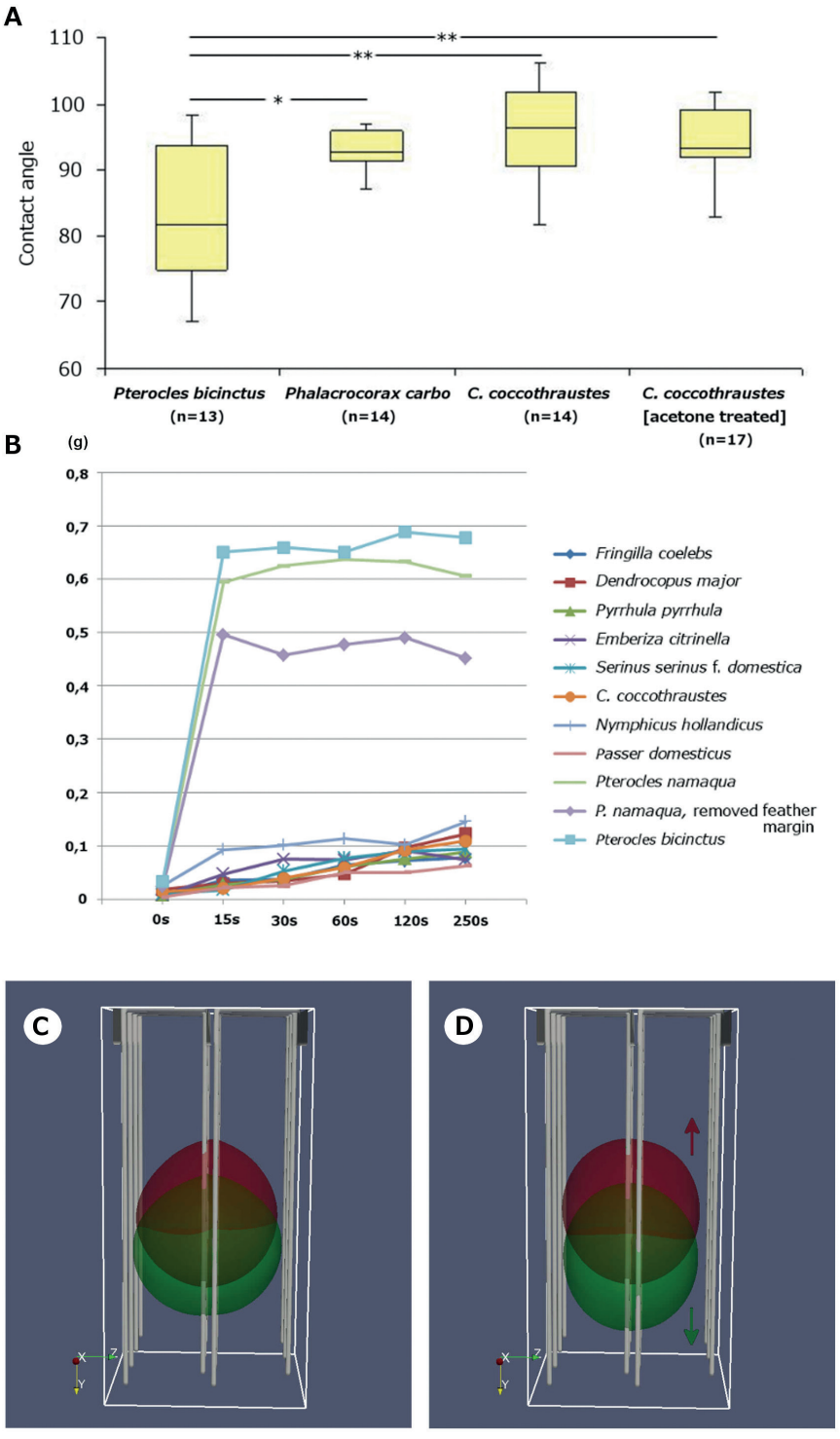

Fig. 7. A. Material contact angle of breast feathers from *P. bicinctus*, *P. carbo* and *C. coccothraustes* (natural condition and treated with acetone) measured by tensiometer. Two-tailed t-test * = $p < 0.05$, ** = $p < 0.01$. **B**. Water absorption capacity during the first 250 s of feathers from sandgrouse and non-sandgrouse species (n = 10 per species). In contrast to the linear water absorption of the non-sandgrouse species over the whole time the sandgrouse show their maximum water uptake already after 15 s. Water absorption of sandgrouse feathers without the outer rim was reduced by about 30%. **C–D**. Overlapped droplet positions (red = sandgrouse-geometry, green=varied geometry) in lateral view of both numerical simulations at t = 1.2 ms (C) and t = 1.8 ms (D). Arrows in D indicate the direction of movement. While the droplet in the sandgrouse-geometry reached a steady state in the structure during the simulation time the droplet in the varied-geometry still fell downwards.

also a large (r+d)/r-value which suggests a poor water-repellent behavior, which is in contrast to non-sandgrouse species. The calculated intrinsic contact angles show so that the breast feathers of the sandgrouse differ from all others comparison species due to their hydrophilicity.

The sandgrouse feathers reached their maximum **water absorption** already within the first 15s and fluctuated afterwards. This contrasts with the much lower and linear increase of water uptake in the non-sandgrouse species which show no adaptations for water transport (feather structure and contact angle). In contrast to Thomas & Robin (1977), who did not have enough data to evaluate their hypothesis, we now demonstrate that the sandgrouse feathers show no evidence for a Michaelis-Menten saturation curve.

In the **numerical simulation** it could be shown that the microstructural parameters are optimized for water absorption. Already a minimal reduction of about 30% of the barbules in the digital geometry results in a strong reduction of the water retaining ability.

We could also show that in the evolution of sandgrouse the pterylography, the macro-, micro- and internal structures of the breast feathers as well as their wetting properties are highly optimized for the water transport which could be thought of as autapomorphy of the family that got subsequently lost in *S. tibetanus* because of its mountainous lifestyle. The evolution of this highly complex mechanism should be further investigated as it is a recent example of a substantial functional change of a complex structure.

Acknowledgements. We thank M. Griebel, H. Schmitz, T. Stegmaier, C. Kaya, A. Scherrieble, H. Roßmaier, L. Pastrik, M. Piefke, A. Hamm, I. Nüssle, R. van den Elzen, D. Stiels, J. Kasimir, K. Völker, M. Hendel, M. Lambertz, P. Comanns and C. Stommel. We would like to thank Dieter Wittmann for the idea for this work. The work was supported by grants from the German Federal Ministry of Education and Research (BMBF) to H.S. and from the German Research Foundation (DFG) to D.K.

REFERENCES

Amat JA, Masero JA (2007) The functions of belly-soaking in Kentish plovers *Charadrius alexandrinus*. Ibis 149: 91–97

Amat JA, Masero JA (2008) Belly-soaking: a behavioural solution to reduce excess body heat in the Kentish plover *Charadrius alexandrinus*. Journal of Ethology 27: 507–510

Begg GW, Maclean GL (1976) Belly-soaking in the White-crowned Plover. The Ostrich 47: 65

Cade TJ, MacLean GL (1967) Transport of water by adult sandgrouse to their young. The Condor 69: 323–343

Cassie ABD, Baxter S (1944) Wettability of porous surfaces. Transactions of the Faraday Society 40: 546–551

Croce R, Griebel M, Schweitzer MA (2010) Numerical simulation of bubble and droplet deformation by a level set approach with surface tension in three dimensions. International Journal for Numerical Methods in Fluids 62: 963–993

de Juana E (1997) Family Pteroclidae (Sandgrouse). Pp 30–57 in: del Hoyo J Elliott A & Sargatal J (eds) Handbook of the Birds of the World, Vol. 4. Sandgrouse to Cuckoos. Lynx Edicions, Barcelona

Dove CJ (1997) Quantification of microscopic feather characters used in the identification of North American plovers. The Condor 99: 47–57

Grant GS (1981) Belly-soaking by Incubating Common, Sandwich, and Royal Terns. Journal of Field Ornithology 52: 244

Goutner V (1984) Belly-soaking in the Avocet. Ostrich 55: 167–168

Jackson JA, Schardien BJ (1981) Belly-soaking as a possible thermoregulatory mechanism in nesting Purple Martin. North American Bird Bander 6: 12–13

Joubert CSW, MacLean GL (1973) The structure of the water-holding feathers of the Namaqua Sandgrouse. Zoologica Africana 8: 141–152

Klocke D, Schmitz H (2012) Material properties of photomechanical infrared receptors in pyrophilous *Melanophila* beetles and *Aradus* bugs. Acta Biomaterialia 8: 3392–3399

Lloyd P, Durrans L, Gous R, Little RM, Crowe TM (2000) The diet and nutrition of the Namaqua sandgrouse, an arid-zone granivore. Journal of Arid Environments 44: 105–122

MacLean GL (1968) Field studies on the sandgrouse of the Kalahari desert. Living Bird 7: 209–235

MacLean GL (1983) Water Transport by Sandgrouse. BioScience 33: 365–369

MacLean GL (1975) Belly-soaking in the Charadriiformes. Journal of the Bombay Natural History Society 72: 74–82

Rijke AM (1970) Wettability and Phylogenetic Development of Feather Structure in Water Birds. The Journal of Experimental Biology 52: 469–479

Rijke AM (1972) The Water-Holding Mechanism of Sandgrouse Feathers. Journal of Experimental Biology 56: 195–200

Sangster G, Braun EL, Johansson US, Kimball RT, Mayr G, Suh A (2022) Phylogenetic definitions for 25 higher-level clade names of birds. Avian Research 13: 100027

Seymour RS, Ackerman RA (1980) Adaptations to Underground Nesting in Birds and Reptiles. American Zoologist 20: 437–447

Sick H (1937) Morphologisch-funktionelle Untersuchungen über die Feinstruktur der Vogelfeder. Journal für Ornithologie 85: 206–372

Sitte P, Ziegler H, Ehrendorfer F, Bresinsky A (1998). Strasburger. Lehrbuch der Botanik (34th ed.). Gustav Fischer Verlag, Stuttgart

Strong CM, Miyako S (2004) Black Skimmers Invade the Bay. Tideline 24: 1–3

Thomas DH, Robin AP (1977) Comparative studies of thermoregulatory and osmoregulatory behaviour and physiology of five species of sandgrouse (Aves: Pterocliidae) in Morocco. Journal of Zoology 183: 229–249

Wenzel RN (1936) Resistance of solid surfaces to wetting by water. Industrial and Engineering Chemistry 28: 988–994